

- <sup>5</sup>E. P. Mazets and Yu. V. Sergeenkov, *Izv. Akad. Nauk SSSR Ser. Fiz.* **30**, 1185 (1966) [transl.: *Bull. Akad. Sci. USSR, Phys. Ser.* **30**, 1237 (1966)].
- <sup>6</sup>E. Knappek, R. Simon, R. S. Raghavan, and H. J. Körner, *Phys. Letters* **29B**, 581 (1969).
- <sup>7</sup>V. Singh, P. N. Tandon, S. H. Devare, and H. G. Devare, *Nucl. Phys.* **A131**, 92 (1969).
- <sup>8</sup>A. Graue, J. R. Lien, S. Røyrvik, O. J. Arrøy, and W. H. Moore, *Nucl. Phys.* **A136**, 513 (1969).
- <sup>9</sup>H. Sergolle, G. Albouy, J. M. Lagrange, M. Pautrat, N. Poffé, and J. H. Vanhorenbeeck, *Nucl. Phys.* **A145**, 351 (1970).
- <sup>10</sup>M. L. Narasimha Raju, V. Seshagiri Rao, and D. L. Sastry, *Phys. Rev. C* **2**, 566 (1970).
- <sup>11</sup>A. Murelius, J. Lindskog, Z. Awwad, K. G. Väilivaara, S. E. Hägglund, and J. Pihl, *Nucl. Phys.* **A148**, 433 (1970).
- <sup>12</sup>D. W. Cruse, K. Johansson, and E. Karlsson, *Nucl. Phys.* **A154**, 369 (1970).
- <sup>13</sup>L. D. Wyly, J. B. Salzberg, E. T. Patronis, Jr., N. S. Kendrick, and C. H. Braden, *Phys. Rev. C* **1**, 2062 (1970).
- <sup>14</sup>L. D. Wyly, J. B. Salzberg, E. T. Patronis, Jr., N. S. Kendrick, and C. H. Braden, *Phys. Rev. C* **3**, 2442 (1971).
- <sup>15</sup>H. M. Perdue and R. A. Meyer, *Bull. Am. Phys. Soc.* **15**, 1668 (1970).
- <sup>16</sup>W. M. Roney and R. R. Borchers, *Bull. Am. Phys. Soc.* **15**, 1676 (1970).
- <sup>17</sup>L. S. Kisslinger and R. A. Sorensen, *Rev. Mod. Phys.* **35**, 853 (1963).
- <sup>18</sup>L. S. Kisslinger, *Nucl. Phys.* **78**, 341 (1966).
- <sup>19</sup>R. J. Blin-Stoyle and M. A. Grace, in *Handbuch der Physik*, edited by H. Geiger and K. Scheel (Springer-Verlag, Berlin, Germany, 1957), p. 555.
- <sup>20</sup>S. R. de Groot, H. A. Tolhoek, and W. J. Huiskamp, in *Alpha-, Beta-, and Gamma-Ray Spectroscopy*, edited by K. Siegbahn (North-Holland Publishing Company, Amsterdam, The Netherlands, 1965), p. 1199.
- <sup>21</sup>K. S. Krane and R. M. Steffen, *Phys. Rev. C* **2**, 724 (1970).
- <sup>22</sup>D. C. Camp and A. L. Van Lehn, *Nucl. Instr. Methods* **76**, 192 (1969).
- <sup>23</sup>J. A. Barclay, W. D. Brewer, E. Matthias, and D. A. Shirley, in *Hyperfine Structure and Nuclear Radiations*, edited by E. Matthias and D. A. Shirley (North-Holland Publishing Company, Amsterdam, The Netherlands, 1968), p. 902.
- <sup>24</sup>J. R. Sites, H. A. Smith, and W. A. Steyert, to be published.
- <sup>25</sup>J. R. Sites and W. A. Steyert, *Nucl. Phys.* **A156**, 19 (1970).
- <sup>26</sup>J. E. Templeton and D. A. Shirley, *Phys. Rev. Letters* **18**, 240 (1967).

## Fission of Heavy Nuclei at Higher Excitation Energies in a Dynamic Model\*

Rainer W. Hasse†

*Physics Division, Oak Ridge National Laboratory, Oak Ridge, Tennessee 37830*

(Received 28 December 1970)

The dynamic model of asymmetric fission used in calculating the mass and kinetic energy distributions of the fragments from thermal-neutron-induced fission of  $^{235}\text{U}$  is employed here to calculate these distributions for fission at higher excitation energies and for other heavy nuclei at low excitation energies. The model itself is investigated with respect to the semi-phenomenological shell correction. It is found that the mass distribution of the fragments in the reaction  $^{235}\text{U}(n, f)$ , which for thermal neutrons is strongly peaked at the heavy-fragment mass 132, goes over into a symmetric mass distribution at a compound-nuclear temperature of about 6 MeV.

### 1. INTRODUCTION

The experimental data associated with symmetric fission of medium-heavy nuclei (lighter than about radium) can be explained rather well in the framework of a dynamic liquid-drop model<sup>1</sup>: The classical Hamiltonian here consists of the potential energies of an incompressible liquid drop, i.e., surface and Coulomb energies, and of the kinetic energy of the irrotational flow of an ideal nonviscous liquid.

After having prescribed some arbitrary family of shapes which is passed through by the nucleus en route to fission, the potential energy is first made stationary to find the saddle point. The de-

formation coordinates are then transformed at the saddle point into a normal coordinate system in order to determine the probability of the system having some initial condition. The equations of motion are then solved for a limited number of initial conditions close to the saddle point up to the scission point. Usually one takes only  $2n+1$  sets of different initial conditions, with  $n$  being the number of deformation or normal coordinates taken into account: one set with all normal coordinates and momenta vanishing, i.e., on top of the saddle; and  $2n$  sets with only one of the normal coordinates or momenta having a small nonzero value.

The smooth dependence of the Hamiltonian on

the deformation coordinates allows one to find with this procedure correlations between the initial conditions at the saddle and the final ones at the scission point. For the  $n - 1$  normal oscillators at the saddle point, the quantum-mechanical probability distributions for the normal coordinates  $\eta_i$  and the normal velocities  $\dot{\eta}_i$  are applicable:

$$\begin{aligned} P(\eta_i) &\propto \exp[-\eta_i^2(\kappa_i/\hbar\omega_i)\tanh(\hbar\omega_i/2\theta)] \\ P(\dot{\eta}_i) &\propto \exp[-\dot{\eta}_i^2(\mu_i/\hbar\omega_i)\tanh(\hbar\omega_i/2\theta)], \\ &i = 1 \cdots n - 1, \quad (1) \end{aligned}$$

where  $\kappa_i$ ,  $\mu_i$ ,  $\hbar\omega_i$  are the normal stiffness, normal effective mass, and curvature of the normal oscillator of the  $i$ th mode, and  $\theta$  is the compound-nuclear temperature. The remaining  $n$ th mode, the fission mode, corresponds to an inverted oscillator, and hence the distributions of Eq. (1) are not valid. Because the fission mode ( $F$ ) is unstable, no normalizable probability distribution exists. One assumes very slow motion in the fission direction and fixes the fission coordinate at the saddle point, and for the fission velocity takes the classical distribution

$$\begin{aligned} P(\eta_F) &\propto 1 \\ P(\dot{\eta}_F) &\propto \exp[-\dot{\eta}_F^2(\mu_F/2\theta)]. \quad (2) \end{aligned}$$

Furthermore, one assumes the final distributions to be of the Gaussian type; thus one can transform the initial distributions with aid of the results of the dynamic calculations into the final ones to obtain distributions, e.g., of the fragment masses and kinetic energies of motion. The experimental distributions of the kinetic energies of the infinitely separated fragments can then be compared with the theoretical ones which consist of distributions of the kinetic energies of motion and the Coulomb interaction energy at the scission points.

## 2. THE MODEL

The dynamic model described in Sec. 1 was successfully applied by Nix and Swiatecki<sup>1</sup> to the symmetric-fission process of medium-heavy nuclei, and the experimentally known data were reproduced rather well. However, the model in this form is not applicable to the asymmetric-fission process of heavy nuclei with low excitation energies. It fails for the reason that the Hamiltonian, and especially its potential energy owing to its internal structure, only favors symmetric nuclear shapes, since shell effects are not taken into account. For asymmetric fission, shell effects become predominant as shown with static calculations.<sup>2</sup>

In previous papers<sup>3</sup> we performed similar dynamic calculations but with inclusion of a semiphenomenological shell-energy correction in order to calculate the asymmetric mass and kinetic energy distributions of the fragments from thermal-neutron-induced fission of <sup>235</sup>U. In addition, we added the curvature energy to the liquid-drop potential.

The shapes used were the so-called generalized spheroids. In cylindrical coordinates  $(\rho, \zeta)$  the three-parameter family in dimensionless form reads

$$\rho^2 = \lambda[\zeta_0^2 - (\zeta + \zeta_s)^2][\zeta_2|\zeta_2| + (\zeta + \zeta_s - \zeta_1)^2]. \quad (3)$$

Here the deformation coordinates  $\zeta_0$ ,  $\zeta_1$ , and  $\zeta_2$  describe elongation, asymmetry, and constriction (necking in), respectively, and have the following features: For  $\zeta_2 \rightarrow \infty$  spheroids with the major and minor semiaxes  $\zeta_0$  and  $\zeta_0^{-1/2}$ , respectively, form a subfamily;  $\zeta_2 = 0$  describes the configuration of (nonspherical) tangent fragments, and  $\zeta_2 < 0$  gives configurations of two separated fragments. Half the length of the nucleus is always  $\zeta_0$  in units of  $R_0 = r_0 A^{1/3}$ . The asymmetry coordinate  $\zeta_1$  is zero for reflection-symmetric shapes and has a finite value which is related to the mass ratio for post-scission shapes or to the reflection asymmetry for pre-scission shapes. The quantities  $\lambda$  and  $\zeta_s$  are eliminated by means of volume conservation and fixing the center of mass.

This parametrization is suitable to describe many kinds of shapes involved in the stages of fission with only three deformation coordinates. In addition, we were able to continue the integration of the equations of motion past the scission point where the half-density radii of the fragments touch each other and to proceed further to the fission point where the densities of the fragments no longer overlap (cf. Ref. 3). The scission point and fission point lie about 1.25 fm apart, which corresponds to about  $\zeta_2 = -0.2$ . Transformation to normal coordinates at the saddle results in two oscillation modes, i.e., vibration ( $V$ ) and asymmetry ( $A$ ), and the unstable fission mode ( $F$ ).

In considering the shell energy to be added we needed a correction which could be written in closed form in order to limit the computer time. Thus it was obvious to take a modified form of the Myers and Swiatecki<sup>4</sup> shell correction which was introduced to reproduce nuclear masses and deformations. This shell energy is a wriggly function of  $N$  and  $Z$  and deformation, but has the property of vanishing for large deformations (about at the saddle point). We, however, wanted to relate the asymmetric mass distribution with the fragment's shells. The modification therefore consisted of adding the shell energies of the two frag-

ments or clusters and multiplying them by an attenuation factor which guarantees that the sum of the shell energies of the fragments will be valid at the scission point and for post-scission shapes and that the approximate value of zero is achieved at the saddle. It reads

$$E_{\text{shell}} = [E_{\text{MS}}(N_{\text{H}}, Z_{\text{H}}) + E_{\text{MS}}(N_{\text{L}}, Z_{\text{L}})] \times \begin{cases} e^{-b\zeta^2} & \text{for pre-scission,} \\ 1 & \text{for post-scission.} \end{cases} \quad (4)$$

Here  $E_{\text{MS}}$  denotes the deformation-independent part of the Myers and Swiatecki shell energy, and  $N_{\text{H}}, Z_{\text{H}}$  or  $N_{\text{L}}, Z_{\text{L}}$  the neutron and proton numbers of the heavy or light fragments or clusters. The definition of the clusters in the case of pre-scission can be found in Ref. 3. The attenuation factor  $e^{-b\zeta^2}$  with its attenuation parameter  $b$ , which is studied below, is arbitrary but is chosen in this way so that the shell energy has the properties required above.

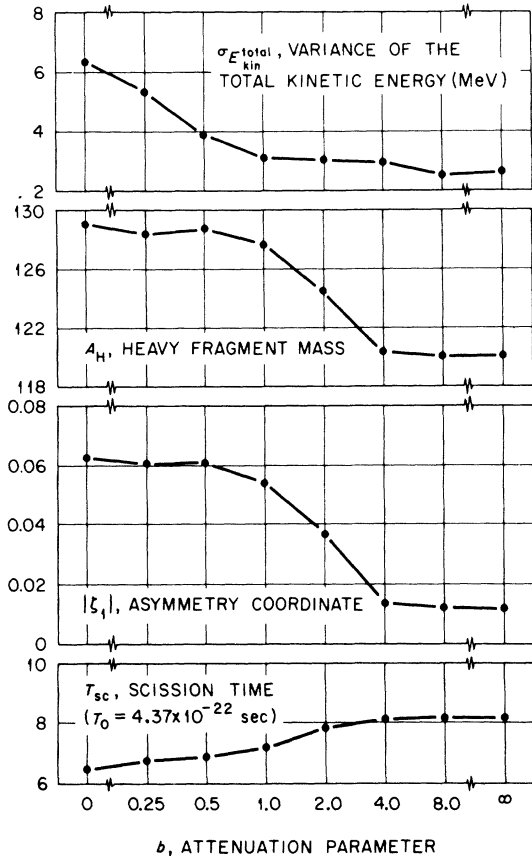


FIG. 1. Average scission time in units of  $T_0$ , absolute value of the asymmetry coordinate, most probable heavy-fragment mass, and average variance of the total kinetic energy of the fragments in thermal-neutron fission of  $^{235}\text{U}$  as a function of the attenuation parameter. Increasing  $b$  means a decreasing shell-energy strength.

The inclusion of the shell energy did complicate the calculations because the dependence of the potential energy on the deformation coordinates is no longer smooth as it is in the pure liquid-drop model. It was impossible to find simple correlations between the initial and final distributions (the latter are no longer of the Gaussian type) and we had, rather, to apply the Monte Carlo method and solve (in general 100 times for one problem) the equations of motion with random initial coordinates.

Let  $k$  be a random integer,  $0 \leq k \leq 9$ ; then the corresponding initial normal coordinate  $\eta$  or the velocity  $\dot{\eta}$  is given according to the Monte Carlo method by

$$\begin{aligned} \eta_i^{(k)} &= r^{(k)} \left( \frac{\hbar\omega_i}{\kappa_i} \coth \frac{\hbar\omega_i}{2\theta} \right)^{1/2}, \\ \dot{\eta}_i^{(k)} &= r^{(k)} \left( \frac{\hbar\omega_i}{\mu_i} \coth \frac{\hbar\omega_i}{2\theta} \right)^{1/2}, \quad i = V \text{ or } A, \\ \eta_F &= 0, \quad \dot{\eta}_F^{(k)} = r^{(k)} \left( \frac{2\theta}{\mu_F} \right)^{1/2} \end{aligned} \quad (5)$$

with  $r^{(k)}$  given implicitly by the error function

$$\text{erf}[r^{(k)}] = \frac{1}{10} k. \quad (6)$$

Furthermore, if  $\bar{r}$  is an average value of  $r^{(k)}$ , e.g.,  $\bar{r} = \frac{1}{10} \sum_k r^{(k)} = 0.47$ , the average total energy in all collective degrees of freedom is

$$E^* = \bar{r}^2 \left( \hbar\omega_V \coth \frac{\hbar\omega_V}{2\theta} + \hbar\omega_A \coth \frac{\hbar\omega_A}{2\theta} + \theta \right),$$

$$E^* \rightarrow \begin{cases} \bar{r}^2 (\hbar\omega_V + \hbar\omega_A) & \text{for } \theta \ll \hbar\omega_i, \\ 5\bar{r}^2 \theta & \text{for } \theta \gg \hbar\omega_i. \end{cases} \quad (7)$$

The scheme described here is slightly different from the one used in the previous papers where we dealt only with thermal-neutron fission. The small nuclear temperatures (taken as being zero) there limited the range of the normal coordinates to the immediate vicinity of the saddle.

### 3. THERMAL-NEUTRON FISSION

The attenuation parameter  $b$  in the attenuation factor  $e^{-b\zeta^2}$  determines the strength of the influence of the shells of the clusters on the pre-scission potential energy. The limiting cases are  $b \rightarrow \infty$ , i.e., no shell energy at all and  $b = 0$ , i.e., the shell energy consists of the full sum of the shell energies of the two clusters. Both cases are unrealistic and a reasonable value should lie in between.

Throughout the previous papers we have used  $b = 1$  which is here justified with the results of the thermal-neutron fission calculations of  $^{235}\text{U}$ . In Fig. 1 the average scission time and absolute value of the asymmetry coordinate at fission and the

most probable heavy-fragment mass and variance of the total kinetic energy are plotted vs the logarithmically scaled attenuation parameter. One can see that up to about  $b=1$  the mean probable heavy-fragment mass has the same value of about 129. This number is close to the doubly magic nucleus  $^{132}_{82}\text{Sn}_{50}$ , which is energetically favored by the shell energy. The average scission time and mean probable variance of the total kinetic energy of the fragments do not show the behavior of having a flat plateau for small attenuation parameters. These quantities are very sensitive to changes in the potential energy: With increasing shell-energy strength valleys appear in the asymmetry degree of freedom of the potential-energy surface. In these valleys the nucleus descends more rapidly than it does in the smooth liquid-drop surface. As a consequence, more energy is put into the symmetric degrees of freedom and the final symmetric deformation coordinates will spread more than in the pure liquid-drop case. Since the kinetic energies of the fragments and their variances due to the electrostatic interaction energy depend more

strongly on the geometrical shapes of the fragments rather than on their mass ratios, the total variances are enhanced. Because of the limited number of degrees of freedom taken into account, the variances come out to be smaller than the experimental ones.

Figure 2 shows the heavy-fragment mass distributions in the fission of  $^{235}\text{U}$  and  $^{241}\text{Pu}$  with thermal neutrons and in the spontaneous fission of  $^{252}\text{Cf}$ , compared with the experimental mass-yield curves.<sup>5</sup> The attenuation parameter here and in the following calculations is equal to unity. The resulting mass distributions are also strongly peaked close to the doubly magic heavy fragment  $^{132}_{82}\text{Sn}_{50}$  rather than at the experimental value of about 140. The peak stays at the same mass number when going to heavier compound nuclei ( $^{236}\text{U}$ ,  $^{242}\text{Pu}$ ,  $^{252}\text{Cf}$ ) but it becomes broader with a very heavy-fragment tail. This effect is not observed experimentally but is easy to explain in the framework of the dynamic model. In the liquid-drop model, heavier nuclei such as  $^{252}\text{Cf}$  have an essentially lower barrier which is more flat than for nuclei such as  $^{236}\text{U}$ . Thus the motion is slower and the final coordinates are more spread in deformation space. Furthermore, as we know from cranking-model calculations<sup>6,7</sup> of the effective masses in the kinetic energy, these are (10 to 20 times) larger than the irrotational values used in our kinetic energy. Hence the influence of the kinetic energy is underestimated and the potential energy is overestimated. This may explain also why the resulting scission times of  $3 \times 10^{-21}$  sec are about  $10^6$  times smaller than estimated from fission widths.<sup>8</sup>

The averages of the kinetic energies of the fragments in Fig. 3 and their variances in Fig. 4 also reflect this discrepancy. The large kinetic energies are shifted to lighter-fragment masses, and their variances increase more rapidly with increasing compound-nuclei masses than measured. The scattering of the theoretical points of the variances in the heavy-fragment tail in the case of  $^{252}\text{Cf}$  comes from poor statistics.

#### 4. FISSION AT HIGHER EXCITATION ENERGIES

Similar calculations were performed for the compound nucleus  $^{236}\text{U}$  with higher excitation energies corresponding to nuclear temperatures up to  $\theta = 7.23$  MeV. Since the excitation energy  $E^*$  does not enter directly in Eqs. (5)–(7), but rather enters implicitly through the nuclear temperature, the dependence of the fragment's distributions on temperature is studied. Conversion formulas from  $\theta$  to  $E^*$  will be given below.

The mass distributions of Fig. 5 show the ex-

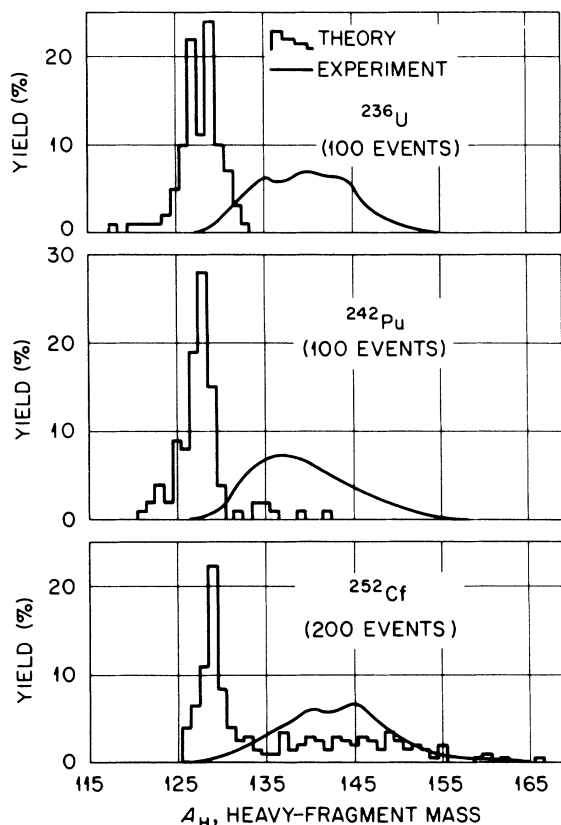


FIG. 2. Histograms of the heavy-fragment mass distributions in thermal-neutron fission of  $^{235}\text{U}$  and  $^{241}\text{Pu}$  and spontaneous fission of  $^{252}\text{Cf}$ . Experimental data are taken from Ref. 5.

pected transition from asymmetry to symmetry with higher temperatures. Simultaneously, they become broader. These two effects are also reflected in the other quantities of interest which are displayed in Fig. 6. The dependences of the most probable heavy-fragment mass and of the average asymmetry coordinate on the temperature are misleading because they are not only composed of the decreasing asymmetry but also of the increasing width. The decreasing asymmetry is predominant for temperatures up to 1.5 MeV. For higher temperatures the rapidly increasing width of the mass distribution also causes the most-probable heavy-fragment mass number to increase.

The inverse relation between scission time and variance of the total kinetic energy is about the same as in their dependence on the attenuation parameter. The decrease in scission time here comes from the higher excitation energy in the collective degrees of freedom. The higher the

energy is, the less the shell wiggles in the asymmetry direction are felt from the system en route from saddle to scission. As a consequence, the motion becomes faster and the distributions of the final coordinates have larger widths.

Experimentally, mass distributions of the fragments from fission of actinide nuclei with light particles are known for a wide variety of bombarding energies: thermal,<sup>5</sup> low and moderate up to about 50 MeV,<sup>9</sup> medium up to about 200 MeV,<sup>10</sup> and high energies up to 28 GeV.<sup>11</sup>

The mass distributions go over continuously from an asymmetric distribution to a symmetric one with a peak-to-valley ratio of unity reached at between 50- and 150-MeV bombarding energy. Simultaneously, the full width at half maximum (FWHM) of each peak increases from about 15 amu (<sup>235</sup>U with thermal neutrons) to 22 amu (<sup>235</sup>U with 15.5-MeV neutrons), 27 amu (<sup>237</sup>Np with 40.5-MeV helium ions, not yet symmetric fission), and the total FWHM of the symmetric mass distribution stays about 55 amu for all higher energies.

In comparing the theory with experiment, the bombarding energy has to be converted into an excitation energy: The bombarding energy equals the excitation energy above the saddle plus fission barrier of the compound nucleus minus the binding energy between the projectile and the target. In fission of actinide nuclei the difference between fission barrier and binding energy of the projectile is negligible (both are on the order of 6 MeV). Thus the excitation energy is about equal to the bombarding energy.

The excitation energy in turn can be converted

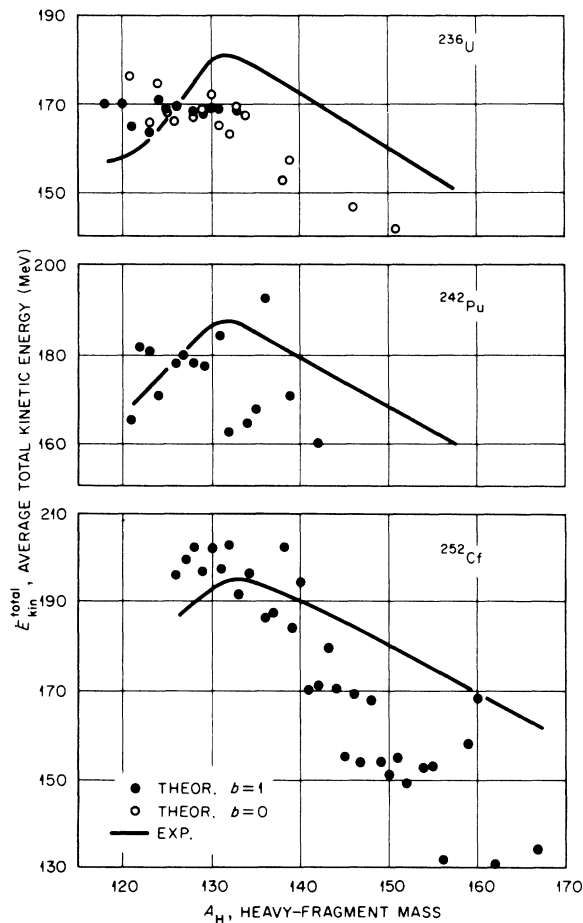


FIG. 3. Distributions of the total kinetic energies of the fragments from thermal-neutron fission of <sup>235</sup>U and <sup>241</sup>Pu and spontaneous fission of <sup>252</sup>Cf. Experimental data are from Ref. 5.

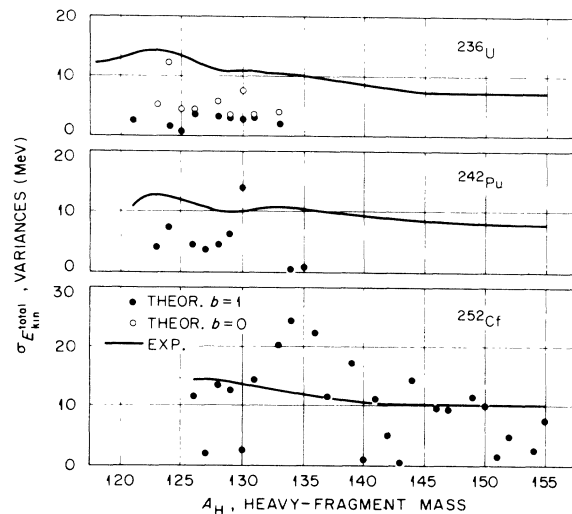


FIG. 4. Variances of the total kinetic energy distributions of the fragments from thermal-neutron fission of <sup>235</sup>U and <sup>241</sup>Pu and spontaneous fission of <sup>252</sup>Cf. Experimental data are from Ref. 5.

to a nuclear temperature with the aid of the semi-empirical formula of Lang and LeCouteur<sup>12</sup>

$$E^* = \frac{A}{8 \text{ MeV}} \theta^2 - \theta, \quad (8)$$

which was obtained by fitting neutron-evaporation spectra with the Fermi-gas equation of state. However, the Fermi-gas model does hold only under the assumption that the energies in a large number of degrees of freedom are in statistical equilibrium. Because we took only into account three collective degrees of freedom and no internal ones, Eq. (8) is not expected to hold accurately. On the other hand, Eq. (7), which assumes all excitation energy to be in the collective degrees of freedom, will overestimate the available collective energy.

Especially the lower limit of  $E^* = 1.47$  MeV for zero temperature, which is fixed by the zero-point energies of the vibration and asymmetry oscillators at the saddle, is subject to an appre-

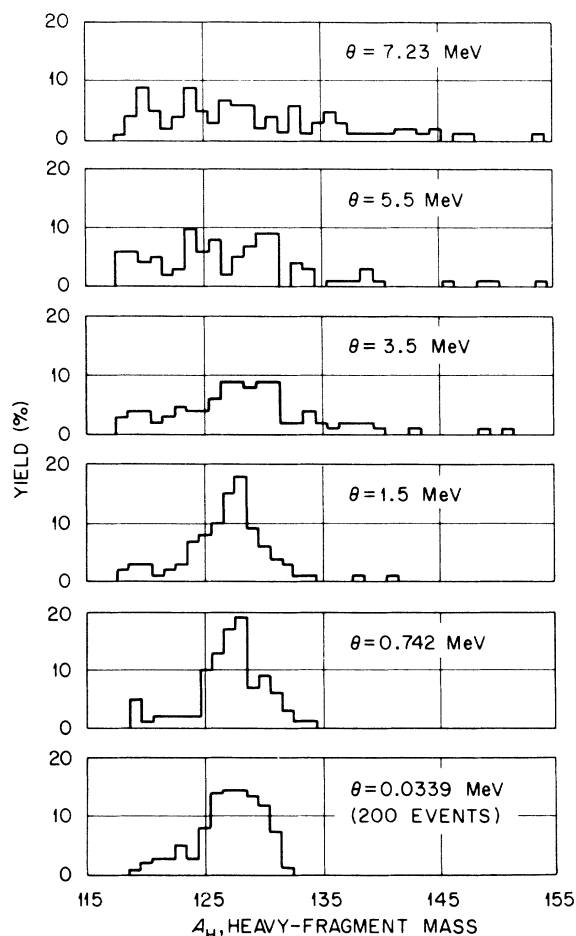


FIG. 5. Histograms of the heavy-fragment mass distributions in fission of  $^{235}\text{U}$  at higher excitation energies as a function of the nuclear temperature.

ciable error. It should be essentially zero for two reasons: (i) At the saddle point, there are indeed more than three collective degrees of freedom available, and application of the statistical Eq. (8) yields  $\theta = 0.0339$  MeV for zero excitation energy; (ii) the liquid-drop mass formula coefficients are fitted without recognizing the zero-point energies. Thus the ground-state energy of a nucleus corresponds to the minimum of the liquid-drop potential-energy surface and the saddle-point energy to the exact top of the saddle. This uncertainty creates an error in the temperatures also on the order of 1.5 MeV, and the temperatures above 1.5 MeV in Figs. 5 and 6 should be corrected by subtracting this value.

This explains why the theoretical mass distributions for temperatures up to 1.5 MeV differ only within the limits of the statistical errors. [As a test of whether the low number of only 100 events yields good statistics, the average excitation energy was calculated according to  $\langle E^* \rangle = \frac{1}{2} \langle \sum_i (\kappa_i \eta_i^2 + \mu_i \tilde{\eta}_i^2) \rangle$  for each temperature, and in Fig. 7 are compared with Eq. (7) (dots vs solid line). The

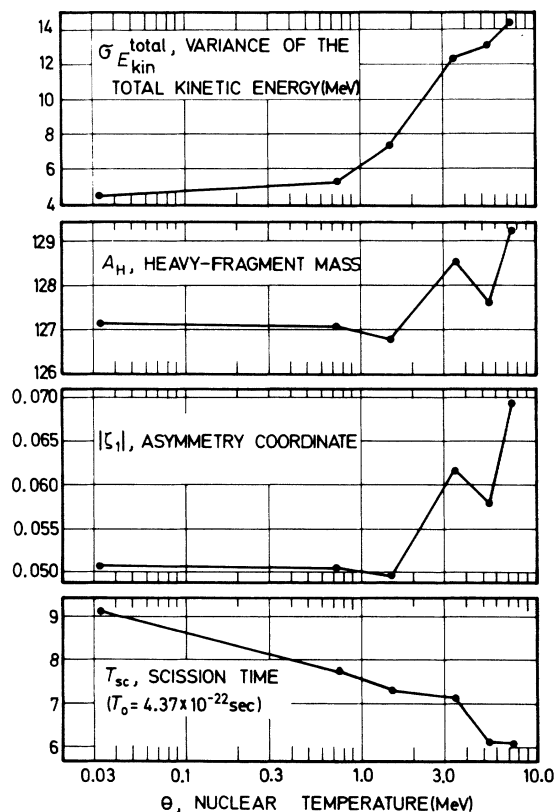


FIG. 6. Average scission time in units of  $T_0$ , absolute value of the asymmetry coordinate, most probable heavy-fragment mass, and average variance of the total kinetic energy of the fragments in fission of  $^{235}\text{U}$  at higher excitation energies.

excellent agreement indicates reasonable statistics.]

The 6-MeV temperature needed to get a symmetric mass distribution now compares with about 600-MeV excitation energy or 5.5-MeV collective excitation energy. This is not in agreement with experiment, but for the reasons discussed above no better agreement was expected.

On the other hand, the theoretical total width of 50–60 amu of the symmetric mass distributions obtained with temperatures above 6 MeV agrees rather well with the experimental one. For such energies, the small shell correction no longer is felt by the system and could be omitted. Thus, the pure liquid-drop model is a good model to work with not only in fission of light and medium-heavy nuclei<sup>1</sup> but also in fission of heavy nuclei with medium and high excitation energies. The width of the mass distribution then is entirely determined by the smooth liquid-drop potential.

## 5. DISCUSSION

There are two major discrepancies between the theoretical results obtained with the dynamic model and the experimental data. (i) The most-probable heavy-fragment mass in low-energy fission comes out to be about 132 rather than 140, and (ii) the transition from asymmetric to symmetric fission is at several hundred MeV excitation energy rather than at about 100 MeV.

The first discrepancy is closely related to the question of whether shell effects at the saddle, at

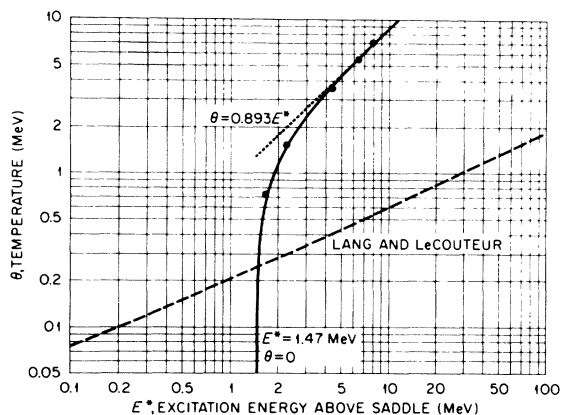


FIG. 7. Correlations between the nuclear temperature and the excitation energy above saddle according to Lang and LeCouteur (Ref. 12), Eq. (8), and according to the formula arrived at if one assumes all excitation energy to be in the collective degrees of freedom Eq. (7). The high and low energy limits of Eq. (7) are also indicated. Dots indicate the average values of the excitation energies achieved in these calculations by 100 random initial sets for each temperature. The compound nucleus considered is  $^{236}\text{U}$ .

scission, or at both points are responsible for the asymmetry of fission. The former assumption can be confirmed by the calculations of Möller and Nilsson or Pauli, Ledergerber, and Brack.<sup>2</sup> These authors obtained asymmetric secondary saddles for compound nuclei which fission asymmetrically, and symmetric ones for symmetrically fissioning nuclei. Furthermore, Moretto and Stella<sup>13</sup> calculated deformation probabilities for higher excitation energies in a statistical model. Their results are that the probability that the compound nucleus will be (symmetrically) deformed decreases with increasing excitation energy. For about  $E^* = 20$  MeV the probability is larger for finding the nucleus in its spherical state than in the deformed ground state. Their conclusion that shell energies are washed out with increasing excitation energy is in agreement with calculations of Damgaard *et al.*<sup>7</sup>

On the other hand, the influence of the doubly magic nucleus  $^{132}_{82}\text{Sn}_{50}$  enters strongly by the fact that experimentally the light sides of the heavy-fragment mass peaks from thermal-neutron fission of  $^{233}\text{U}$ ,  $^{235}\text{U}$ ,  $^{239}\text{Pu}$ , and  $^{241}\text{Pu}$  are almost congruent and located at  $A_H = 132$ , and that the total fragment kinetic energies are peaked at this value.<sup>14</sup> For higher excitation energies not only the mass distributions become symmetric but also the total kinetic energy distributions.<sup>15</sup> This indicates that also the fragment's shells are washed out with excitation. Primary shells at the scission point (such as  $Z = 50$  and  $N = 82$ ), however, cannot be responsible for the most-probable heavy-fragment mass at  $A_H = 140$ . Either secondary shells in the deformed fragments or shells in the compound system of the two tangent fragments with their densities and potential wells still overlapping may explain this phenomenon.

As a result, it is likely that shell effects at the saddle as well as at the scission point and in between must be considered in a sound theory of fission of heavy nuclei.

The semiphenomenological ansatz for the shell energy in the calculations above does not allow for shell effects at the saddle. Secondary shells in deformed fragments are not contained in the model either, since the parametrization of shapes employed is too restricted near the scission point and since nuclear interaction between the fragments is neglected. Due to these restrictions, the calculated low-energy-fragment mass distribution peaks at  $A_H = 132$  rather than at 140 and the low-energy total fragment kinetic energies seem to peak at symmetry rather than at 132.

As regards the second discrepancy mentioned above, the irrotational effective masses are most likely responsible for the high excitation energies

needed to obtain a symmetric mass distribution. The use of more realistic cranking masses or allowance for viscosity of the nuclear matter and/or vorticity of the flow will enhance the internal kinetic energy. (Recently, Schirmer<sup>16</sup> gave a method to calculate the viscosity coefficients, and applied it to nuclei with deformations of the generalized spheroid type.) Furthermore, the attenuation of the shell effects with increasing excitation energy was disregarded up to now. It could be incorporated into the model by multiplying the shell energy, Eq. (4), by the attenuation factor  $e^{-c\theta}$  with  $c \approx 2 \text{ MeV}^{-1}$  or by making the attenuation parameter  $\theta$  temperature dependent. Cranking masses, viscosity, vorticity, and the attenuation of shell effects with increasing excitation energy would result in symmetric fragment mass distributions at lower excitation energies.

## 6. SUMMARY

In using the liquid-drop model with semiphenomenological shell effects and applying the Monte Carlo method, we calculated mass distributions and related quantities in fission of actinide nuclei with excitation energies ranging from zero up to 1.7 GeV.

For low-energy fission, the mass distributions are strongly asymmetric at a most-probable heavy-fragment mass close to the doubly magic nucleus  $^{132}\text{Sn}$ . For higher excitations, the fragment mass distributions become symmetric at a nuclear temperature of 6 MeV. Thus, the model qualitatively, although not quantitatively, describes these nuclear-fission processes. Symmetric fission of light and medium-heavy nuclei can be described by the pure liquid-drop model without

shell effects.

There are indications that using more realistic shell energies and effective masses and allowing for viscosity and vorticity may result in better quantitative agreement with experiment. However, dynamic calculations are limited by the capacity of the presently available electronic computers. Although the Coulomb energies (three-fold integrals) and the effective masses for deformed shapes were calculated in advance at about 30 000 grid points and recalled from magnetic tape into the  $1500 \times 10^3$ -bytes memory of the Oak Ridge IBM 360/91 computer and the equations of motion were solved by interpolating between the grid points, it takes about 20 min of computer time to obtain one mass distribution of 100 events. Thus, presently, there is no hope of performing more complex dynamic calculations.

## ACKNOWLEDGMENTS

This work was started at the Physikalisches Institut der Universität Würzburg with a research grant from the Bundesministerium für Wissenschaftliche Forschung. Most of it was performed during the author's stay at the Physics Division of the Oak Ridge National Laboratory with a NATO fellowship which is gratefully acknowledged. He appreciates the kind hospitality extended to him. Fruitful discussions with Dr. H. W. Schmitt, Dr. F. Plasil in Oak Ridge, Dr. J. R. Nix in Los Alamos, and Dr. W. J. Swiatecki and Dr. W. D. Myers in Berkeley were very helpful and are much appreciated. The author thanks Dr. H. W. Schmitt for a reading of the manuscript and Dr. E. Hilf for presenting parts of this paper at the 1969 Vienna conference.

\*Research partially sponsored by the U. S. Atomic Energy Commission under contract with the Union Carbide Corporation.

†NATO fellow, on leave of absence from the Physikalisches Institut der Universität Würzburg, Würzburg, Germany. Present address: Institut für Theoretische Physik der Universität Heidelberg, Abteilung für Kernphysik, 69 Heidelberg, Germany.

<sup>1</sup>J. R. Nix and W. J. Swiatecki, Nucl. Phys. **71**, 1 (1965); J. R. Nix, *ibid.* **A130**, 241 (1969).

<sup>2</sup>P. Möller and S. G. Nilsson, Phys. Letters **31B**, 283 (1970); H. C. Pauli, T. Ledergerber, and M. Brack, Phys. Letters **34B**, 264 (1971).

<sup>3</sup>R. W. Hasse, R. Ebert, and G. Süßmann, Nucl. Phys. **A106**, 117 (1968); R. W. Hasse, *ibid.* **A118**, 577 (1968); Phys. Letters **27B**, 605 (1968); Nucl. Phys. **A128**, 609 (1969); in *Proceedings of the Second International Symposium on the Physics and Chemistry of Fission, Vienna, Austria, 1969* (International Atomic Energy Agency,

Vienna, Austria, 1969), p. 33.

<sup>4</sup>W. D. Myers and W. J. Swiatecki, Nucl. Phys. **81**, 1 (1966); Arkiv Fysik **36**, 343 (1967).

<sup>5</sup>H. W. Schmitt, J. H. Neiler, and F. J. Walter, Phys. Rev. **141**, 1146 (1966); J. H. Neiler, F. J. Walter, and H. W. Schmitt, *ibid.* **149**, 894 (1966).

<sup>6</sup>C. Y. Wong, Nucl. Data **A4**, 271 (1968); S. G. Nilsson, C. F. Tsang, A. Sobczewski, Z. Szymański, S. Wycech, C. Gustafson, I.-L. Lamm, P. Möller, and B. Nilsson, Nucl. Phys. **A131**, 1 (1969).

<sup>7</sup>J. Damgaard, H. C. Pauli, V. M. Strutinsky, C. Y. Wong, M. Brack, and A. Stenholm-Jensen, in *Proceedings of the Second International Symposium on the Physics and Chemistry of Fission, Vienna, Austria, 1969* (International Atomic Energy Agency, Vienna, Austria, 1969), p. 213.

<sup>8</sup>D. Popovitch, in *Proceedings of the United Nations International Conference on the Peaceful Uses of Atomic Energy, Geneva, 1955* (United Nations, New York, 1956),



Vol. 2, p. 164.

<sup>9</sup>J. A. Powers, N. A. Wogman, and J. W. Cobble, *Phys. Rev.* **152**, 1096 (1966); P. P. Dyachenko, B. D. Kuzminov, and M. Z. Tarasko, *Yadern. Fiz.* **8**, 286 (1968) [transl.: *Soviet J. Nucl. Phys.* **8**, 165 (1969)]; I. F. Croall and J. B. Cunningham, *Nucl. Phys.* **A125**, 402 (1969).

<sup>10</sup>P. C. Stevenson, H. G. Hicks, W. E. Nervi, and D. R. Nethaway, *Phys. Rev.* **111**, 886 (1958); A. C. Pappas and E. Hagebø, *J. Inorg. Nucl. Chem.* **28**, 1769 (1966); A. C. Pappas, *Z. Naturforsch.* **21a**, 995 (1966).

<sup>11</sup>G. Friedlander, in *Proceedings of the International Symposium on the Physics and Chemistry of Fission, Vienna, Austria, 1965* (International Atomic Energy Agency, Vienna, Austria, 1965), Vol II, p. 265; L. P. Remsberg, F. Plasil, J. B. Cumming, and M. L. Perl-

man, *Phys. Rev.* **187**, 1597 (1969).

<sup>12</sup>J. M. B. Lang and K. J. LeCouteur, *Proc. Phys. Soc. (London)* **A67**, 586 (1954); J. K. LeCouteur and D. W. Lang, *Nucl. Phys.* **13**, 32 (1959).

<sup>13</sup>L. G. Moretto and R. Stella, *Phys. Letters* **32B**, 558 (1970).

<sup>14</sup>H. W. Schmitt, in *Proceedings of the Second International Symposium on the Physics and Chemistry of Fission, Vienna, Austria, 1969* (International Atomic Energy Agency, Vienna, Austria, 1969), p. 67.

<sup>15</sup>A. I. Obukhov and A. Perfilov, *Usp. Fiz. Nauk* **92**, 621 (1967) [transl.: *Sov. Phys. - Usp.* **10**, 559 (1968)].

<sup>16</sup>J. Schirmer, Diploma thesis, München, 1970 (unpublished).

PHYSICAL REVIEW C

VOLUME 4, NUMBER 2

AUGUST 1971

## Nuclear Structure of the $N = 82$ Isotones\*

W. P. Jones,† L. W. Borgman,‡ K. T. Hecht, John Bardwick, and W. C. Parkinson  
*Cyclotron Laboratory, Department of Physics, The University of Michigan, Ann Arbor, Michigan 48105*

(Received 8 April 1971)

The nuclear structure of the  $N = 82$  isotones  $Ba^{138}$ ,  $La^{139}$ ,  $Ce^{140}$ ,  $Pr^{141}$ , and  $Nd^{142}$  has been studied using the single-proton-transfer reactions  $(He^3, d)$  and  $(d, He^3)$  on  $La^{139}$ ,  $Ce^{140}$ , and  $Pr^{141}$  targets. Distorted-wave analysis of the angular distributions has been used to determine angular momentum transfers and spectroscopic factors for states up to about 3-MeV excitation. The experimental data are compared with recent shell-model calculations, and in particular with the results of calculations using a new simplifying coupling scheme, the pseudo spin-orbit coupling scheme.

### I. INTRODUCTION

From the point of view of the nuclear shell model there is considerable evidence that systems with 50 and 82 nucleons form particularly stable systems, that both  $N = 82$  and  $Z = 50$  are "good" closed shells. Thus, there is reason to expect that the properties of the low-lying states of the  $N = 82$  isotones should be explainable in terms of configurations of the remaining  $(Z - 50)$  protons. These excess protons should be filling, predominantly, the  $1g_{7/2}$ ,  $2d_{5/2}$ ,  $2d_{3/2}$ ,  $3s_{1/2}$ , and  $1h_{11/2}$  single-particle orbits.

Proton-transfer reactions such as  $(He^3, d)$  and  $(d, He^3)$  are particularly well suited for studying the nature of the low-lying levels of such nuclei, since they either add or take away a proton from the target nucleus and thus should excite strongly only those states, where the proton configurations have a good overlap with those in the ground state of the target nucleus. These reactions are selective as to the character of the state they populate, and as a result the total number of states excited is relatively small. Further, the nature of the reaction mechanism is sufficiently well understood

that it is possible to extract from the experimental data much of the spectroscopic information necessary for a theoretical study of the nuclear structure in this region of the Periodic Table. Such information includes the energy of the states, their spins and parities, and the intrinsic strengths (spectroscopic factors) of the various transitions which in turn provide information on the occupation probabilities of the shell-model orbits.

In the experimental work reported here the low-lying levels of  $Ba^{138}$ ,  $La^{139}$ ,  $Ce^{140}$ ,  $Pr^{141}$ , and  $Nd^{142}$  have been investigated by means of the  $(He^3, d)$  and/or the  $(d, He^3)$  reaction. Additional proton-transfer data are now available<sup>1</sup> on the same family of  $N = 82$  isotones for  $I^{135}$ ,  $Cs^{137}$ ,  $Pm^{143}$ , and  $Eu^{145}$ , as well as some data from  $(n, \gamma)$ ,  $\beta$  decay,  $(\gamma, \gamma')$  and inelastic proton, deuteron, and  $\alpha$ -particle scattering.

A recent shell-model calculation<sup>2</sup> taking into account the complete  $g_{7/2}$ ,  $d_{5/2}$  configurations of the  $(Z - 50)$  protons with some excitation into the  $s_{1/2}$ ,  $d_{3/2}$  orbits has met with considerable success in explaining the data on the positive-parity levels. Recent calculations using quasiparticle techniques